Streamlined Loads Analysis of Floating Wind Turbines With Fiber Rope Mooring Lines

Preprint

Matthew Hall, Brian Duong, and Ericka Lozon

National Renewable Energy Laboratory

Presented at the ASME 2023 5th International Offshore Wind Technical Conference
Exeter, England
December 18–19, 2023

NREL is a national laboratory of the U.S. Department of Energy
Office of Energy Efficiency & Renewable Energy
Operated by the Alliance for Sustainable Energy, LLC

This report is available at no cost from the National Renewable Energy Laboratory (NREL) at www.nrel.gov/publications.

Contract No. DE-AC36-08GO28308

Conference Paper
NREL/CP-5000-87481
January 2024

Streamlined Loads Analysis of Floating Wind Turbines With Fiber Rope Mooring Lines

Preprint

Matthew Hall, Brian Duong, and Ericka Lozon

National Renewable Energy Laboratory

Suggested Citation
Hall, Matthew, Brian Duong, and Ericka Lozon. 2024. *Streamlined Loads Analysis of Floating Wind Turbines With Fiber Rope Mooring Lines: Preprint*. Golden, CO: National Renewable Energy Laboratory. NREL/CP-5000-87481.
https://www.nrel.gov/docs/fy24osti/87481.pdf.

NREL is a national laboratory of the U.S. Department of Energy
Office of Energy Efficiency & Renewable Energy
Operated by the Alliance for Sustainable Energy, LLC

This report is available at no cost from the National Renewable Energy Laboratory (NREL) at www.nrel.gov/publications.

Contract No. DE-AC36-08GO28308

Conference Paper
NREL/CP-5000-87481
January 2024

National Renewable Energy Laboratory
15013 Denver West Parkway
Golden, CO 80401
303-275-3000 • www.nrel.gov

NOTICE

This work was authored by the National Renewable Energy Laboratory, operated by Alliance for Sustainable Energy, LLC, for the U.S. Department of Energy (DOE) under Contract No. DE-AC36-08GO28308. Funding provided by U.S. Department of Energy Office of Energy Efficiency and Renewable Energy Wind Energy Technologies Office. The views expressed herein do not necessarily represent the views of the DOE or the U.S. Government. The U.S. Government retains and the publisher, by accepting the article for publication, acknowledges that the U.S. Government retains a nonexclusive, paid-up, irrevocable, worldwide license to publish or reproduce the published form of this work, or allow others to do so, for U.S. Government purposes.

This report is available at no cost from the National Renewable Energy Laboratory (NREL) at www.nrel.gov/publications.

U.S. Department of Energy (DOE) reports produced after 1991 and a growing number of pre-1991 documents are available free via www.OSTI.gov.

Cover Photos by Dennis Schroeder: (clockwise, left to right) NREL 51934, NREL 45897, NREL 42160, NREL 45891, NREL 48097, NREL 46526.

NREL prints on paper that contains recycled content.

STREAMLINED LOADS ANALYSIS OF FLOATING WIND TURBINES WITH FIBER ROPE MOORING LINES

Matthew Hall*, Brian Duong, Ericka Lozon

National Renewable Energy Laboratory
15013 Denver West Parkway, Golden, CO 80401 USA

ABSTRACT

This paper presents an approach for more accurate yet relatively streamlined accounting for the nonlinear characteristics of synthetic fiber rope mooring lines for floating wind turbines. First, we select a minimal set of parameters that can efficiently approximate a mooring line material's quasi-static and dynamic stiffness characteristics. We also develop a set of baseline coefficients for different rope materials based on published product information and research papers. We then expand a quasi-static mooring model to include dynamic mooring line stiffness terms in a way that allows the nonlinear stiffness behavior of fiber ropes to be considered even in quasi-static analyses. For dynamic analysis, we have updated the model MoorDyn, coupled with OpenFAST, to work with the new dynamic mooring line stiffness terms. This includes the implementation of a new viscoelastic approach that allows the tension-strain relation of each mooring line segment to vary between two stiffness values, depending on the strain rate. After presenting the formulation of the approaches for modeling synthetic ropes, they are demonstrated on a floating wind turbine mooring system with taut polyester rope mooring lines. The results are compared with those of other approaches of similar fidelity, including the static-dynamic method and separate simulations with static and dynamic stiffness values. Comparing the results shows the ability of the new method to match the results of the previous methods in a more streamlined manner.

Keywords: mooring system, synthetic rope, elasticity, polyester, mooring model

1. INTRODUCTION

Mooring systems for floating wind turbines often include synthetic fiber rope mooring lines to benefit from their elasticity and minimal weight. These fiber rope mooring systems are especially helpful in deep waters, where the low weight of synthetic lines is essential. Unlike chain or wire rope, synthetic fiber mooring lines provide restoring force due to the stiffness of the rope, rather than the weight. Therefore, accurately understanding and modeling the elasticity of fiber mooring lines is essential. However, fiber mooring lines have complex stiffness properties that are nonlinear and time-dependent, and these characteristics are not well represented in commonly used mooring system modeling tools. Using these tools to simulate the dynamic response of fiber rope mooring lines within a floating wind system generally entails neglecting known nonlinear rope behaviors or conducting multiple simulations to properly evaluate a single load case.

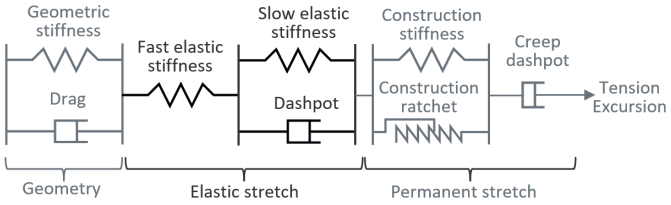

FIGURE 1: MODEL OF ROPE STIFFNESS MECHANISMS (ADAPTED FROM DNV-RP-305 [2])

This paper presents developments that allow for including nonlinear characteristics of fiber rope mooring lines in a streamlined workflow using open-source modeling tools. The elastic properties of fiber rope mooring lines depend on a variety of factors—including loads applied at the moment, load history, and load amplitude—making it difficult to define stiffness characteristics [1]. Multiple nonlinear phenomena are at play, including a one-time installation stretch, slow creep over time, a generally nonlinear quasi-static tension-strain response, and viscoelastic behavior in which the slope of the tension-strain relation depends on the strain rate. The most dominant of these phenomena are illustrated in Figure 1.

For the mooring models considered in this work, a mooring line's geometric stiffness (the first block in Figure 1) is directly accounted for in the model. We neglect irreversible stretch behaviors such as construction stretch and creep as outside the scope of this work, and outside the timescale of any single loads analysis. We therefore focus on the elastic stretch component in Figure 1.

*Corresponding author: matthew.hall@nrel.gov

With this focus, a mooring line's elastic behavior within a given load case can be simplified into two extremes: a static (or slow) stiffness and a dynamic (or fast) stiffness.

Generally speaking, static stiffness can be understood as the stiffness of a tension member when it is loaded slowly, leaving time for the morphology of the material to react to the load. Dynamic stiffness is the stiffness response when a mooring line is under cyclic loading at a fast enough frequency that the amorphous part of the line has no time to react, leaving the crystalline part to take on the load, resulting in a stiffer response [3].

When considering fiber ropes of different sizes, a rope's stiffness characteristics generally scale in proportion to the rope's minimum breaking load (MBL). It is common to quantify a stiffness coefficient, k_r, that is normalized by MBL and therefore constant for different-sized ropes of the same composition:

$$k_r = EA/MBL, \tag{1}$$

where EA is the mooring line stiffness coefficient, with the same units as MBL. Subscripts can be added to distinguish static or dynamic stiffness quantities.

A rope's dynamic stiffness often depends on multiple factors. The American Bureau of Shipping guidelines for fiber ropes recommend the following equation for the normalized dynamic stiffness coefficient:

$$K_{rd} = \alpha + \beta L_m + \gamma L_a + \delta \log(P), \tag{2}$$

where α is a constant stiffness term, β represents a linear increase in stiffness with mean load (L_m), γ is an additional increase in stiffness with load amplitude (L_a), and δ is a further increase with load period (P). Studies such as [4] have found that some of these terms can be neglected for some rope types.

The most significant nonlinear effect for most applications is how a floating system's maximum offsets are governed by a lower stiffness value, related to the ropes' slow-acting stiffness behavior, while the maximum mooring line tensions are driven by the effective stiffness of the mooring lines in response to fast-acting motions/strains. Because both offsets and tensions are typically key design constraints, the fundamental challenge is to model the mooring lines in a way that can accurately represent both behaviors.

There are several common approaches to account for a synthetic rope's varying stiffness, as illustrated in Figure 2. The **upper-lower bound method** assumes two linear stiffness values that represent the minimum and maximum expected stiffness [5]. The minimum stiffness value is used to calculate the maximum platform offset, and the maximum stiffness value is used to calculate maximum line tensions. This method is easy to implement; however, it is thought to be overly simplistic and not reflective of the complicated stiffness properties of fiber ropes. It can result equally in overconservative or nonconservative predictions.

The **nonlinear stiffness method** represents the dynamic stiffness of fiber lines by assuming that the dynamic stiffness is a function of the mean load [5]. This results in a nonlinear tension-strain curve, as shown in Figure 2. The drawback of this approach is that it only considers dynamic stiffness for the complete response. In reality, fiber lines respond to static loads very differently—with

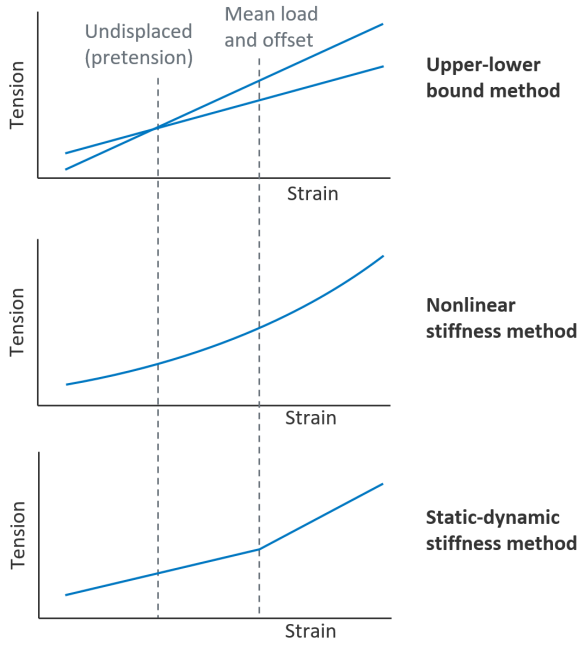

FIGURE 2: TYPICAL METHODS FOR HANDLING SYNTHETIC ROPE STIFFNESS

stiffness values that are approximately half of dynamic stiffness in the case of polyester. Therefore, this approach is expected to underpredict maximum platform offsets, which are an important constraint in the design of mooring systems.

Finally, the **static-dynamic stiffness method** uses a bilinear tension-strain relation [6]. In this approach, the static stiffness is used up until the mean load or mean offset strain. Beyond that point, the dynamic stiffness is used to account for the larger dynamic tension peaks that occur during cyclic loading around the mean load. This piecewise combination of static and dynamic stiffness values allows use of the correct stiffness coefficient when computing both the mean platform offsets and the maximum mooring line tensions. A complication when using the method is that the mean offset and tension varies depending on the load case, so the tension-strain curve may need to be adjusted between cases.

Modeling of static and dynamic stiffness properties for fiber rope mooring lines is widely discussed in the literature. Wibner et al. [7] characterize the polyester rope properties for mooring an FPSO (floating production, storage, and offloading) vessel in deep water. They consider results from full-scale qualification tests to confirm the polyester rope axial stiffness and creep properties, and they propose recommended upper and lower bounds for polyester rope dynamic stiffness coefficients. François et al. [8] present results from extensive testing of the load-elongation properties of polyester ropes and propose a model that considers static and dynamic stiffnesses separately. They consider a nonlinear quasi-static tension-elongation relation and a linearized dynamic stiffness coefficient that is a function of mean load. They also present some results from other fiber ropes, including nylon and high-modulus polyethylene (HMPE) and note that less data is available for these rope materials.

Flory et al. [4] investigated synthetic fiber rope stretch and introduced the idea of accumulated elastic stretch, which causes temporary stretching and stiffening of the rope during tension cycling at high mean loads. They propose that accumulated elastic stretch can have a significant effect during storm conditions and should be considered to accurately determine maximum platform offsets and line tensions. Depalo et al. [1] studied the effects of dynamic rope stiffness on the response of a point absorber wave energy converter for both nylon and polyester mooring systems. They compared a quasi-static stiffness approach with a dynamic amplitude-dependent approach and found that the quasi-static approach underpredicted maximum tensions by 30–40%.

Some studies give insights into the application of different approaches in time-domain simulations. Tahar et al. [9] demonstrate a static-dynamic stiffness approach in the time domain using the dynamic analysis tool CHARM3D. They first compute the stretched length using the static stiffness and then complete a dynamic analysis using the dynamic stiffness and the updated line length. Comparing the static-dynamic method and the upper-lower bound method, the authors found that the upper-lower bound method was overly conservative for both maximum tensions and mean offsets. Pham et al. [10] use an approach that includes both mean load and load amplitude when computing the dynamic stiffness coefficient. They propose an iterative approach for converging on the correct values of these terms based on the standard deviation of tension. The Syrope model [11] implements a capability for dynamically representing the nonlinear and viscoelastic characteristics of ropes in a dynamics model, rather than relying on manual adjustment of linearized coefficients. Aside from this example, models that support viscoelastic represent rope properties are rare, and none are known to be available in open-source simulation tools. Loads analyses for floating wind systems still typically rely on multiple simulations, using different choices of linearized coefficients.

In this study, we establish an open-source solution for modeling fiber rope mooring lines through two main contributions: choosing a set of coefficients for representing the elastic characteristics of synthetic fiber ropes, and updating open-source quasi-static and dynamic mooring models to use and apply these coefficients. We demonstrate the quasi-static and dynamic mooring stiffness models in a case study to provide a comparison of their effects and demonstrate that our single-simulation approach can give comparable results to approaches that require multiple simulations.

2. METHODOLOGY

2.1 Mooring Line Properties

Choosing mechanical property assumptions for mooring lines is an important part of modeling mooring systems, and a variety of assumptions are embedded in different tools and used in different studies. We have gathered product specification sheets and assumptions in published papers in an attempt to synthesize typical property coefficients that can provide a safe and generally applicable reference set. The coefficients are selected in a relative way so that they can be used to calculate the absolute properties of any mooring line as a function of its diameter. The coefficients include standard quantities for weight and strength, along with several values that describe the stiffness properties.

As a practical approach to the complexities of fiber rope elastic characteristics, the coefficient set includes terms for a mooring line material's quasi-static stiffness and dynamic stiffness, with the latter varying linearly with mean tension, reflecting the first two terms in 2.

Our goal in this work is to have a set of properties that can be easily used in loads analyses for floating wind applications. Dependence of properties on mean loads is practical to include because each simulation in a loads analysis typically has a clear mean state that can be determined dynamically during the simulation or ahead of time using a variety of approximation or iteration methods. Dependence of properties on load amplitudes is more challenging to account for because the response amplitudes typically vary stochastically over the length of a simulation, meaning that these properties would be time-varying within a single simulation and their proper calculation would be more involved and prone to uncertainty. For these reasons, we focus only on property coefficients that act on non-time-varying simulation properties.

After an averaging and selection process, we have come up with a baseline set of coefficients for three mooring line materials: polyester, nylon, and high-modulus polyethylene (HMPE). These coefficients are listed in Table 1 and are part of an updated set of default mooring line property assumptions that are included with the MoorPy library.

TABLE 1: SELECTED MOORING LINE COEFFICIENTS

Coefficient	Polyester	Nylon	HMPE
m/d^2 (kg/m/m^2)	798	648	453
d_{vol}/d (-)	0.86	0.85	1.01
MBL/d^2 (MN/m^2)	170.5	164	619
k_{rs} (N/m^2)	14	5	56.5
$k_{rd}\alpha$ (N/m^2)	14	1	59
$k_{rd}\beta$ (N/m^2)	0.34	0.3	0.54

2.2 Adjusting the Unstretched Length

A key step when applying methods that involve changing stiffness values is the calculation of an adjusted value for the line's unstretched length such to match the correct tensions in the mean offset position. To derive this correction, we consider a mooring line connected to a floating platform at its mean offset position. For simplicity, we also approximate that the mooring line has a uniform strain over its weight and no net weight so that it also has an even tension distribution.

Under the quasi-static stiffness scenario, the stretched length of the mooring line is

$$L^* = L_0 + \Delta L \tag{3}$$

where L_0 is its unstretched length and ΔL is its elongation. The line tension is then

$$\tau = \frac{\Delta L}{L_0} EA \tag{4}$$

where EA is the quasi-static stiffness coefficient.

We now want to switch to a dynamic stiffness coefficient, EA', without disrupting the current state of the line at the mean

offset position. Therefore, we need to maintain the same stretched length (which determines the line profile) and tension. The corresponding equalities based on equations (3 and 4) are:

$$L^* = L_0 + \Delta L = L_0' + \Delta L' \tag{5}$$

$$\tau = \frac{\Delta L}{L_0} EA = \frac{\Delta L'}{L_0'} EA' \tag{6}$$

where the prime symbol indicates the value corresponding to the new EA value.

These equations can be solved to obtain an expression for the required new unstretched length:

$$L_0' = \frac{L_0 + \Delta L}{1 + \frac{EA}{EA'}\frac{\Delta L}{L_0}} = \frac{L_0 + \Delta L}{1 + \frac{\tau}{EA'}} = L_0 \frac{1 + \tau/EA}{1 + \tau/EA'}. \tag{7}$$

This provides the adjustment of the unstretched length needed to give the same line state at the current position.

This approach is approximate because a mooring line's tension is rarely exactly constant of its length, and therefore its strain varies. An iterative approach could be used to achieve an exact tension match. However, because fiber ropes typically have a very small apparent weight, the tension and strain variation over a rope mooring line is usually very small, and so iteration is likely unnecessary.

2.3 Quasi-Static Modeling of Rope Elasticity

Both static and dynamic stiffness behaviors of ropes can be included in quasi-static mooring models. These models are useful in the design process because their quick computation speed allows for rapid design exploration and use in the loop of optimization routines. The quasi-static mooring developed by the National Renewable Energy Laboratory and used in its floating array design tools is MoorPy [12]. MoorPy is based on standard quasi-static catenary equations for mooring lines but includes support for an expanded set of edge cases (such as taut vertical lines or fully slack lines). It has a general form that allows analysis of multiple coupled floating bodies, and it uses an analytical approach to system stiffness matrices, allowing for excellent accuracy and efficiency. MoorPy is available as an open-source Python library.

MoorPy is sometimes used to assess the characteristics of mooring systems in dynamic scenarios. For instance, extreme platform offsets found from dynamic simulations can be applied to MoorPy to estimate the peak mooring system tension (including with a "dynamic amplification factor" to approximate dynamic tension contributions) [13]. In addition, MoorPy is used to model the mooring system in RAFT (Response Amplitudes of Floating Turbines), a frequency-domain dynamics model [14]. In both of these applications, MoorPy's existing linear quasi-static mooring line elasticity characteristics are used when estimating dynamic tensions relative to a mean operating point. If a dynamic stiffness value was instead used, determined based on the line strain or load at the mean offset, then MoorPy could include the tension contribution due to dynamic stiffness in a manner consistent with one of the methods listed in Section 1.

To apply the updated stiffness coefficients, the quasi-static mooring model within MoorPy has been expanded to include dynamic mooring line stiffness terms. When MoorPy evaluates a floating system's equilibrium state and mean tensions, the quasi-static stiffness term is used, consistent with the previous version. However, when MoorPy calculates a mooring system's stiffness matrix and tension derivatives to estimate dynamic responses, the mooring system can be revised to use the dynamic stiffness values that correspond to the mean tensions at the offset position. To preserve the correct line profiles and tensions, (7) is used to adjust each line's unstretched length. This overall process allows the nonlinear stiffness behavior of fiber ropes to be considered even in quasi-static analyses.

The specifics of this process are as follows:

- Store static and dynamic stiffness values for each mooring line
- Find system offset equilibrium under desired load using quasi-static stiffness properties
- Switch to dynamic stiffness values, and adjust the reference unstretched length of each mooring line to preserve the tensions previously calculated in the offset position
- Compute dynamic characteristics about the mean offset such as maximum tension at maximum offset, mooring system stiffness (for system natural frequencies), and mooring tension Jacobians (for tension dynamics in frequency domain)
- When considering another load case or offset position, revert to the static stiffnesses and reset the line unstretched lengths.

The key calculation in performing the process is computing the adjusted unstretched, as was described in Section 2.2.

2.4 Dynamic Modeling of Rope Elasticity

The dynamic mooring model MoorDyn coupled with OpenFAST has also been updated to work with the new dynamic mooring line stiffness terms. This includes the implementation of a new viscoelastic approach that allows the tension-strain relation of each mooring line segment to vary between two stiffness values, depending on the strain rate. This capability works in tandem with the ability to use a user-specified nonlinear tension-strain curve [15], which allows MoorDyn to recreate the variation of dynamic stiffness with mean load.

The MoorDyn viscoelastic implementation works by replacing MoorDyn's usual spring-damper segments with two spring-damper pairs that are in series. Consider two desired stiffnesses, the static k_S and dynamic k_D. A spring system can achieve the static stiffness as motion frequency approaches zero and the dynamic stiffness at higher frequencies by having two spring-dampers in series. Figure 3 shows a mooring line segment arranged this way, with a spring and damper in parallel (k_1 and c_1), connected with another parallel spring-damper pair (k_2 and c_2).

Considering a static state, the dampers will have no effect on the forces, and then the effective stiffness of the combined double spring-damper assembly will be

$$\frac{1}{k_e} = \frac{1}{k_1} + \frac{1}{k_2}. \tag{8}$$

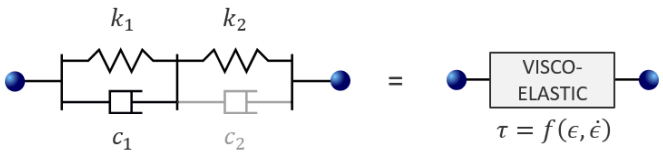

FIGURE 3: BASIC MOORDYN VISCOELASTIC SEGMENT

To simplify for clarity in the following formulation, we neglect the second damper (assume $c_2 = 0$) until later. This allows the effect of c_1 on the segment's frequency response to be easily studied. For very slow motions ($\dot{\epsilon} \rightarrow 0$), the damper will have minimal force contribution, and the stiffness of the segment will be close to the static stiffness value (8). For very fast motions ($\dot{\epsilon} >> 0$), the damper will produce a very large force and essentially lock the first part of the segment, making the stiffness of the segment close to only the second spring, k_2.

The approach for achieving viscoelastic behavior in the MoorDyn line segments is to choose the spring values to achieve the desired static and dynamic stiffness characteristics, with the damper value controlling the frequency-dependent transition between them.

We denote k_S and k_D to be the desired static and dynamic stiffness values of a line segment. To achieve these values, we set

$$k_2 = k_D \tag{9}$$

$$k_1 = \frac{k_S k_D}{k_D - k_S} \tag{10}$$

where the latter equation is simply a rearrangement of (8) with $k_{effective} = k_s$.

After some derivation using common vibration theory methods, we found the effective stiffness of the segment as a function of frequency (ω):

$$k_e(\omega) = |\frac{\tau(\omega)}{\Delta l(\omega)} = k_2 \sqrt{\frac{k_1^2 + \omega^2 c^2}{(k_1 + k_2)^2 + \omega^2 c^2}}. \tag{11}$$

An important quantity with this approach is the frequency at which the stiffness transitions between the static and dynamic values. This can be found from

$$\omega_{half} = \frac{k_1 + k_2}{c} \sqrt{\frac{(k_1 + \frac{1}{2}k_2)^2 - k_1^2}{(k_1 + k_2)^2 + (k_1 + \frac{1}{2}k_2)^2}} \tag{12}$$

The damper value c_1 can be chosen to achieve a desired ω_{half} value so that a simulated mooring system has the desired threshold separating the types of platform motions that generate a response at the static stiffness versus the dynamic stiffness.

A key part of implementing the viscoleastic segment in the time domain is tracking the strain or extension of the two spring-damper pairs. Figure 4 shows the breakdown of tension forces (τ) on each element in the assembly and the extension Δl of each spring-damper pair. The original or unstretched length of the segment does not need to be considered until converting between stiffness (k) and line stiffness coefficient (EA) values.

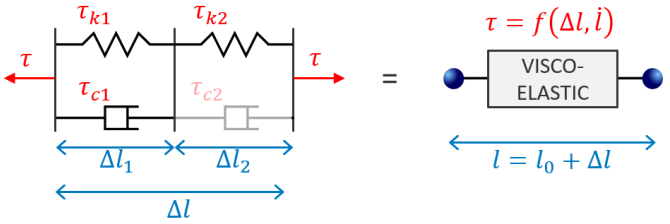

FIGURE 4: TENSIONS AND ELONGATIONS IN THE MOORDYN VISCOELASTIC SEGMENT

Because the viscoelastic segment runs between two nodes in a lumped-mass model, there is no mass associated with the segment itself. This means the total tension at each part of the section is the same and equal to the summed tension of a paired spring and damper. In terms of the symbols labeled in Figure 4, we have

$$\tau = \tau_{k1} + \tau c1 = \tau_{k2} + \tau c2, \tag{13}$$

where $\tau_{k1} = k_1 \Delta l_1$ and $\tau_{c1} = c_1 \dot{l}_1$, with $\dot{l}$ is the rate of change of l (which is the same as the rate of change of Δl). The expanded form of 14 is

$$\tau = k_1 \Delta l_1 + c_1 \dot{l}_1 = k_2 \Delta l_2 + c_2 \dot{l}_2 \tag{14}$$

In MoorDyn, the equations of motion depend on the position, velocity, and acceleration of each node along a mooring line. This requires each node's position and velocity to be states that are integrated in time. The new viscoelastic segment divides up the change in distance between two nodes into two portions, and that division means that the equations of motion now depend also on the extension and extension rate of change of the sections. As a result, one additional state needs to be tracked per segment. We choose Δl_1 as the state to track, meaning that calculation of its derivative needs to be added to the equations of motion. From the information in Figure 4 and (4), the state derivative is

$$\dot{l}_1 = \frac{k_2 \Delta l - (k_2 + k_1)\Delta l_1 + c_2 \dot{l}}{c_2 + c_1} \tag{15}$$

The terms in this equation can be converted to MoorDyn's standard cross-section values of EA and BA as follows:

$$\dot{l}_1 = \frac{EA_2 \Delta l - (EA_2 + EA_1)\Delta l_1 + BA_2 \dot{l}}{BA_2 + BA_1} \tag{16}$$

Adding this state to the MoorDyn equations of motion completes the viscoelastic implementation in the lumped-mass dynamic model.

3. RESULTS

To test the effectiveness of the implemented rope elasticity approaches, we use a case study of a floating wind turbine with a taut polyester rope mooring system. A taut all-rope mooring configuration has the least presence of dynamic effects in the mooring line tensions except for those arising from the elasticity. Hall et al. [16] showed that a tension-leg mooring system had very similar mooring line tensions regardless of whether a quasi-static or dynamic mooring model was used, whereas catenary mooring

configurations showed large differences. That study considered only linear stiffness, and those findings are corroborated for a taut spread mooring system in the results that follow. However, when nonlinear elasticity is included, the tension results change considerably. These characteristics make a taut mooring system well suited for isolating the nonlinear elasticity effects of concern in this study, while minimizing the influence of other phenomena such as hydrodynamic loads.

The floating system used for the case study is the UMaine VolturnUS-S semisubmersible and IEA 15-MW reference floating wind turbine [17]. The properties of this floating system are already widely known. However, the catenary mooring system has been replaced with a taut polyester rope mooring system. This mooring system was designed using in-house mooring optimization tools (similar to those described in [13]), and its properties are listed in Table 2. Table 3 lists the properties of the polyester rope used in the mooring system.

TABLE 2: MOORING SYSTEM CONFIGURATION

Property	Value
Number of lines	3
Water depth (m)	800
Anchoring radius (m)	1800
Fairlead radius (m)	58
Fairlead depth (m)	14
Pretension (kN)	973
Declination angle (deg)	26.5
Section 1 type	Polyester rope
Section 1 unstretched length (m)	1893

TABLE 3: POLYESTER ROPE SECTION PROPERTIES

Property	Value
Volume-equivalent diameter (m)	0.1301
Linear mass (kg/m)	18.25
Minimum breaking load, MBL (kN)	7182
Transverse drag coefficient	1.2
Axial drag coefficient	0.2

The mooring system's design is not important to this work except that it is a roughly reasonable design in terms of its behavior. The mooring line declination angle is 26.5 degrees in the undisplaced position, with a line pretension of 973 kN. The mean offset under the 15-MW turbine's rated thrust force is approximately 33 m.

The results are compared with those of other approaches of similar fidelity, including the static-dynamic method and separate simulations with static and dynamic stiffness values. Comparing the results shows the ability of the new method to match the results of the previous methods in a more streamlined manner.

3.1 Stiffness Method Comparisons in OpenFAST

To demonstrate the behavior of the dynamic modeling of polyester elasticity, we conducted several OpenFAST simulations of the taut-polyester mooring system. These simulations used steady wind at the rated wind speed of 10.59 m/s, resulting in the maximum turbine thrust force and thus the highest loads on the mooring lines. The simulations also included irregular waves aligned with the wind direction, with a significant wave height of 8 m and a wave period of 12.7 seconds. In all simulations, the mooring system was orientated with one mooring line directly upwind, and two mooring lines at a 60° from downwind. The stiffness modeling methods used in the OpenFAST simulations are described in the following list:

- **Static**: this most basic case simply uses the static stiffness value as determined by k_{rs}.
- **Dynamic**: this case switches to the dynamic stiffness value as determined by k_{rd} without any adjustment to the line unstretched lengths.
- **Dynamic with pretension adjustment**: this case uses the dynamic stiffness value as determined by k_{rd} but also adjusts the line unstretched lengths to match the mooring system's pretensions when the platform is in its undisplaced position.
- **Dynamic with tension adjustment**: this case uses the dynamic stiffness value as determined by k_{rd} and adjusts each line's unstretched length to match the mean tension when the platform is in its mean offset position for the given load case.
- **Viscoelastic**: this case uses the viscoelastic capability in MoorDyn to account for both the static and dynamic tension values without requiring any load-case specific adjustment of line unstretched lengths.

For the above modeling methods, the calculated EA and line length values are shown in Table 4. L1 refers to the directly upwind mooring line, while L2 and L3 refer to the mooring lines that are oriented 60° from downwind. The dynamic stiffness is a function of the mean load on the mooring line, so the upwind and downwind lines have different EAs depending on the method. Similarly, the line adjustment relies on the EA of the line, so the upwind and downwind lines have different adjusted lengths in some cases.

TABLE 4: MOORING LINE UNSTRETCHED LENGTH AND EA FOR EACH CASE

	Length (m)		EA (MN)	
Case	Line 1	Line 2/3	Line 1	Line 2/3
Static	1893.0	1893.0	101	101
Dynamic	1893.0	1893.0	191	114
Dyn. w/ preten adj.	1902.0	1893.8	191	114
Dyn. w/ ten adj.	1916.3	1893.3	191	114
viscoelastic	1893.0	1893.0	191*	114*

* The viscoelastic method also uses the static EA of 101 MN.

Figure 5 shows time series results of platform surge and line tensions with the various elastic stiffness methods. The dynamic method predicts the lowest surge and the highest upwind tensions, as this method employs the largest EA value without a line length adjustment. The dynamic method with the pretension adjustment shows a platform surge and line tension in the middle of the

range. This is because the high dynamic stiffness is used, but with a small length adjustment that relies on the mooring system pretension. The static method, the viscoelastic method, and the dynamic stiffness with the mean tension adjustment show the highest surge and the lowest upwind line tensions. This is because the mean upwind tensions are much higher than the pretensions, so the line length adjustment is more significant and the behavior ultimately is closer to the static stiffness.

Looking at the line tensions more closely, the static stiffness method shows the smallest peaks in the upwind line tensions. This is because the static stiffness is the lowest EA, allowing more elongation of the lines and reducing the tension increase. The line tensions for the viscoelastic method and the dynamic stiffness with the mean tension adjustment are the closest, but the viscoelastic model shows slightly smaller peaks in most cases. These line tension peaks are driven by a combination of slow drift motions and fast wave frequency motions, and so the viscoelastic approach will see a lower stiffness for the slow drift component, potentially causing the slightly lower tension amplitudes.

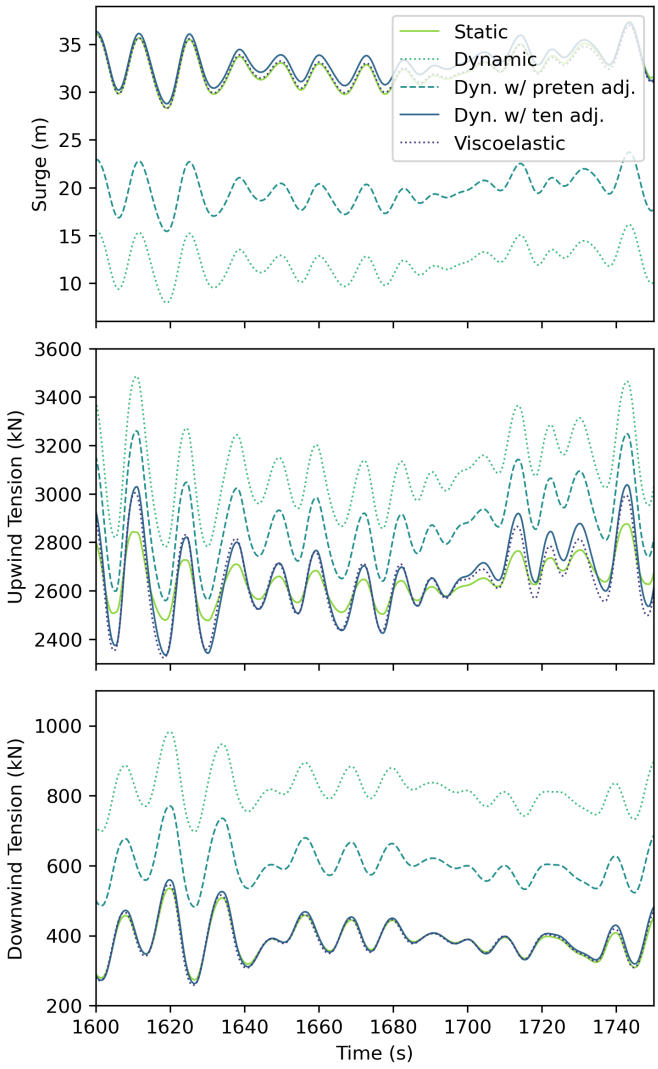

FIGURE 5: PLATFORM SURGE AND LINE TENSIONS WITH VARIOUS STIFFNESS METHODS

Statistics of the platform surge and line tensions for the various elasticity methods are shown in Table 5. The statistics are reflective of the time series, showing higher mean and maximum surge for the static, viscoelastic, and dynamic with mean tensions adjustment methods. Across the methods, the viscoelastic and the dynamic stiffness with mean tensions adjustment show the lowest standard deviation in mooring line tensions. This suggests that these models are adequately capturing the higher stiffness around wave-frequency motions. Looking at the extremes, the static method increases the maximum platform offset by 130% and decreases the maximum tension by 20% from the dynamic stiffness method. The maximum platform offset and line tensions are the main constraints in the design of mooring systems. These results point to the significant impacts of elasticity modeling methodology on the key parameters of tension and offset, highlighting the importance of this study.

TABLE 5: STATISTICS OF PLATFORM SURGE AND MOORING LINE TENSIONS FROM EACH STIFFNESS METHOD

	Mean	Max.	Min.	Std. dev.
Platform Surge (m)				
Static	32.6	37.4	28.3	1.4
Dynamic	12.1	16.2	7.4	1.3
Dyn. w/ preten adj.	19.6	23.7	15.0	1.3
Dyn. w/ ten adj.	33.1	37.3	28.5	1.3
Viscoelastic	32.6	37.0	28.3	1.3
Upwind Tension (kN)				
Static	2645	2875	2447	69
Dynamic	3084	3485	2647	126
Dyn. w/ preten adj.	2866	3259	2433	125
Dyn. w/ ten adj.	2651	3037	2226	123
Viscoelastic	2645	3004	2285	108
Downwind Tension (kN)				
Static	383	535	274	35
Dynamic	815	982	688	41
Dyn. w/ preten adj.	601	771	478	40
Dyn. w/ ten adj.	390	559	263	40
Viscoelastic	383	546	258	38

To further understand the dynamic results, we can compare the tension and stretched line length for the various methods in Figure 6. The dynamic method oscillates around the lowest stretched line length, corresponding to the underpredicted surge offsets known to occur with this method. The dynamic method is also centered around the highest tension of all the methods. The dynamic method with pretension adjustment increases the average stretched line length, but this method still has lower offsets and higher tensions than the rest. The static, viscoelastic, and dynamic-with-mean-tension-adjustment methods all have similar stretched line lengths. The static method, however, clearly has a less-steep slope than the other methods, and the peak tensions are lower. This causes the smaller amplitude tension peaks for the static method, as seen in the time series. The viscoelastic and dynamic method with mean tension adjustment have similar tension to stretched line length patterns, with the dynamic mean tension method generally showing slightly higher peaks. These results provide another view of how the viscoelastic method can give

similar results as the dynamic method with tension adjustments, while requiring only one simulation.

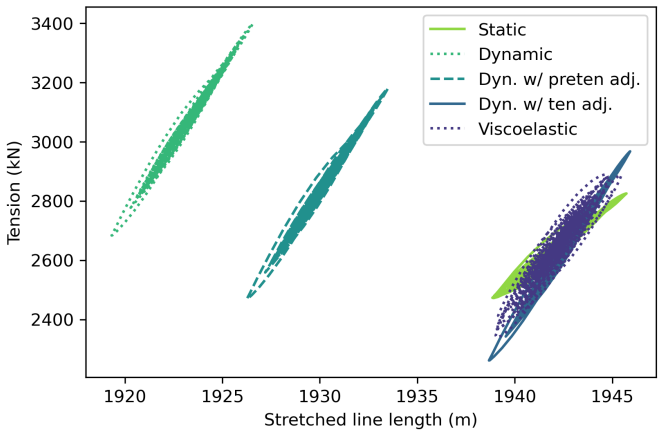

FIGURE 6: UPWIND LINE TENSION AND STRETCHED LENGTH WITH VARIOUS STIFFNESS METHODS

3.2 Comparison With Quasi-Static MoorPy Results

The same mooring system scenario was studied in MoorPy to test the method described in Section 2.3. The mooring system at its undisplaced and mean offset positions is shown in Figure 7.

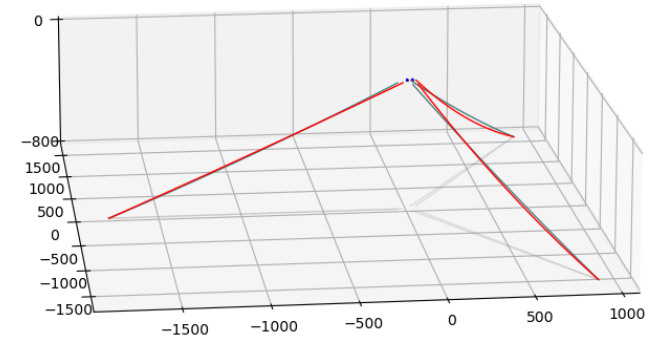

FIGURE 7: MOORPY MOORING SYSTEM IN UNDISPLACED AND MEAN DISPLACED POSITIONS

The process was to set up the mooring system with the static stiffness value and confirm the expected offsets after applying the turbine thrust force value of approximately 2 MN. This achieved the expected mean offset to within 1 m of the OpenFAST results. Next, the maximum surge offset seen from the OpenFAST results was imposed, and the resulting upwind line tension was recorded. This is an estimation of the maximum mooring line tension as seen in the OpenFAST results when using the static stiffness.

Then the system was returned to equilibrium, and the method of switching to dynamic line stiffnesses (and adjusted lengths) was applied. The mooring line tensions at equilibrium were again checked, and the offset was confirmed to be within 1 m of the target. Lastly, the maximum offset from the OpenFAST results was again imposed, and the new line tension recorded. This corresponds to the maximum tension from OpenFAST when using the tension-adjusted dynamic stiffness approach and also the viscoelastic approach.

A comparison of the results between MoorPy and OpenFAST is shown in Table 6. As can be seen, there is good agreement in all cases. This confirms the general validity of the implemented quasi-static approach for this type of mooring system.

TABLE 6: COMPARISON OF PLATFORM SURGE AND MOORING LINE TENSIONS FROM MOORPY VS. MOORDYN

	MoorDyn		MoorPy	
	Mean	Max.	Mean	Max.
Platform Surge (m)				
Static	32.60	37.40	32.44	37.40
Viscoelastic	32.60	36.99	32.61	36.99
Upwind Tension (kN)				
Static	2645	2875	2528	2775
Viscoelastic	2645	3004	2530	2926

4. CONCLUSIONS

The nonlinear and viscoelastic nature of polyester mooring line stiffness is critical in the design and analysis of mooring systems. This paper outlined methodologies to model the stiffness of polyester mooring lines both quasi-statically and dynamically, while considering both the higher dynamic stiffness and the lower static stiffness of the polyester material. The stiffness modeling methodologies are applied to a taut mooring system for a floating offshore wind turbine and compared to traditional upper-lower bound methods.

Results from this work show that using the dynamic stiffness and adjusting the line length based on the mean tension produces results very similar to a viscoelastic method. Meanwhile, using either the dynamic or static stiffness alone results in large under- or over-predictions of peak tensions and platform offsets. The results from the viscoelastic model showed slightly lower amplitudes in line tensions compared to the dynamic mean tension-adjusted model, suggesting that tuning is required to account for low-frequency slow-drift motions. Further, the comparison of peak tensions showed that the choice of elasticity modeling technique can more than double the maximum platform offset and impact peak line tensions by 20%. Given that the extreme line tensions and platform offsets are major drivers in the design of mooring systems, the importance of accurate modeling of polyester mooring lines is essential.

Future work will expand the analysis to consider additional wind/wave directions and load cases, compare against additional elasticity modeling methods, and try the approach on other rope types. The end goal is to characterize the suitability of each method and to provide the methods and guidance so that the most suitable method can be used for a given application.

ACKNOWLEDGMENTS

This work was authored by the National Renewable Energy Laboratory, operated by the Alliance for Sustainable Energy, LLC, for the U.S. Department of Energy (DOE) under Contract No. DE-AC36-08GO28308. Funding provided by the U.S. Department of Energy Office of Energy Efficiency and Renewable

Energy Wind Energy Technologies Office. The views expressed in the article do not necessarily represent the views of the DOE or the U.S. Government. The U.S. Government retains and the publisher, by accepting the article for publication, acknowledges that the U.S. Government retains a nonexclusive, paid-up, irrevocable, worldwide license to publish or reproduce the published form of this work, or allow others to do so, for U.S. Government purposes.

REFERENCES

[1] F. Depalo, S. Wang, S. Xu, C. G. Soares, S.-H. Yang, and J. W. Ringsberg, "Effects of dynamic axial stiffness of elastic moorings for a wave energy converter," *Ocean Engineering*, vol. 251, p. 111132, 2022.

[2] "DNV-RP-E305 RP design, testing and analysis of offshore fibre ropes," tech. rep., 2015.

[3] A. B. of Shipping, "The application of fiber rope for offshore mooring," tech. rep., American Bureau of Shipping, Houston, Texas, June 2021.

[4] J. F. Flory, S. P. Banfield, and D. J. Petruska, "Defining, measuring, and calculating the properties of fiber rope deepwater mooring lines," in *Offshore Technology Conference*, pp. OTC–16151, OTC, 2004.

[5] C. T. Kwan, P. Devlin, P.-L. Tan, and K. Huang, "Stiffness Modeling, Testing, and Global Analysis for Polyester Mooring," in *OMAE2012*, (Volume 1: Offshore Technology), pp. 777–785, July 2012.

[6] ABS, "Guidance notes on the application of fiber rope for offshore mooring," *ABS 90-2011*, 2011.

[7] C. Wibner, T. Versavel, and I. Masetti, "Specifying and testing polyester mooring rope for the barracuda and caratinga fpso deepwater mooring systems," in *Offshore Technology Conference*, pp. OTC–15139, OTC, 2003.

[8] M. Francois, P. Davies, F. Grosjean, and F. Legerstee, "Modelling fiber rope load-elongation properties-polyester and other fibers," in *Offshore Technology Conference*, OnePetro, 2010.

[9] A. Tahar, D. Sidarta, and A. Ran, "Dual Stiffness Approach for Polyester Mooring Line Analysis in Time Domain," in *OMAE2012*, (Volume 1: Offshore Technology), pp. 513–521, July 2012.

[10] H. Pham, P. Cartraud, F. Schoefs, T. Soulard, and C. Berhault, "Dynamic modeling of nylon mooring lines for a floating wind turbine," *Applied Ocean Research*, vol. 87, pp. 1–8, June 2019.

[11] E. Falkenberg, V. Åhjem, and L. Yang, "Best practice for analysis of polyester rope mooring systems," OnePetro, May 2017.

[12] M. Hall, S. Housner, S. Sirnivas, and S. Wilson, "MoorPy (Quasi-Static mooring analysis in python)," 2021. DOI: 10.11578/DC.20210726.1.

[13] M. Hall, E. Lozon, S. Housner, and S. Sirnivas, "Design and analysis of a ten-turbine floating wind farm with shared mooring lines," *Journal of Physics: Conference Series*, vol. 2362, p. 012016, Nov. 2022. Publisher: IOP Publishing.

[14] M. Hall, S. Housner, D. Zalkind, P. Bortolotti, D. Ogden, and G. Barter, "An Open-Source Frequency-Domain model for floating wind turbine design optimization," *Journal of Physics: Conference Series*, vol. 2265, p. 042020, May 2022.

[15] E. Lozon, M. Hall, P. McEvoy, S. Kim, and B. Ling, "Design and analysis of a Floating-Wind Shallow-Water mooring system featuring polymer springs," in *ASME 2022 International Offshore Wind Technical Conference*, American Society of Mechanical Engineers, Oct. 2022.

[16] M. Hall, B. Buckham, and C. Crawford, "Evaluating the importance of mooring line model fidelity in floating offshore wind turbine simulations," *Wind Energy*, vol. 17, pp. 1835–1853, Dec. 2014.

[17] C. Allen, A. Viscelli, H. Dagher, A. Goupee, E. O. Gaertner, N. Abbas, M. Hall, and G. O. Barter, "Definition of the UMaine VolturnUS-S reference platform developed for the IEA wind 15-Megawatt offshore reference wind turbine," Tech. Rep. NREL/TP-5000-76773, National Renewable Energy Lab. (NREL), Golden, CO (United States), July 2020.